

1 **Reconsidering the role of carbonate ion concentration in**
2 **calcification by marine organisms**

3

4 **L. T. Bach¹**

5 [1]{GEOMAR Helmholtz Centre for Ocean Research Kiel, 24105 Kiel, Germany}

6 Correspondence to: L. T. Bach (lbach@geomar.de)

7

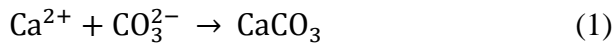
8 **Abstract**

9 Marine organisms precipitate 0.5-2.0 gigaton of carbon as calcium carbonate (CaCO_3) every
10 year with a profound impact on global biogeochemical element cycles. Biotic calcification
11 relies on calcium ions (Ca^{2+}) and generally on bicarbonate ions (HCO_3^-) as CaCO_3 substrates
12 and can be inhibited by high proton (H^+) concentrations. The seawater concentration of
13 carbonate ions (CO_3^{2-}) and the CO_3^{2-} -dependent CaCO_3 saturation state (Ω_{CaCO_3}) seem to be
14 irrelevant in this production process. Nevertheless, calcification rates and the success of
15 calcifying organisms in the oceans often correlate surprisingly well with these two carbonate
16 system parameters. This study addresses this dilemma through rearrangement of carbonate
17 system equations which revealed an important proportionality between $[\text{CO}_3^{2-}]$ or Ω_{CaCO_3} and
18 the ratio of $[\text{HCO}_3^-]$ to $[\text{H}^+]$. Due to this proportionality, calcification rates will always
19 correlate equally well with $[\text{HCO}_3^-]/[\text{H}^+]$ as with $[\text{CO}_3^{2-}]$ or Ω_{CaCO_3} when temperature,
20 salinity, and pressure are constant. Hence, $[\text{CO}_3^{2-}]$ and Ω_{CaCO_3} may simply be very good
21 proxies for the control by $[\text{HCO}_3^-]/[\text{H}^+]$ where $[\text{HCO}_3^-]$ would be the inorganic carbon
22 substrate and $[\text{H}^+]$ would function as calcification inhibitor. If the “substrate-inhibitor ratio”
23 (i.e. $[\text{HCO}_3^-]/[\text{H}^+]$) rather than $[\text{CO}_3^{2-}]$ or Ω_{CaCO_3} controls biotic CaCO_3 formation then some
24 of the most common paradigms in ocean acidification research need to be reviewed. For
25 example, the absence of a latitudinal gradient in $[\text{HCO}_3^-]/[\text{H}^+]$ in contrast to $[\text{CO}_3^{2-}]$ and
26 Ω_{CaCO_3} could modify the common assumption that high latitudes are affected most severely by
27 ocean acidification.

28

29 **1 Introduction**

30 Calcium carbonate (CaCO_3) is used by a large variety of marine organisms as structural
31 material for their exo-and endoskeletons. Calcification requires calcium ions (Ca^{2+}) and
32 dissolved inorganic carbon (DIC) substrate, which is present in seawater as carbon dioxide
33 (CO_2), bicarbonate ion (HCO_3^-) and carbonate ion (CO_3^{2-}). From a purely chemical point of
34 view, calcium reacts with inorganic carbon as:



37

38 Precipitation is thermodynamically favored when $[\text{Ca}^{2+}]$ and $[\text{CO}_3^{2-}]$ reach or exceed the
39 solubility of CaCO_3 in seawater. The stoichiometric solubility product is defined as:

40

$$41 \quad K_{\text{sp}}^* = [\text{Ca}^{2+}]_{\text{saturated}} [\text{CO}_3^{2-}]_{\text{saturated}} \quad (2)$$

42

43 and is a function of temperature, salinity, and pressure (Mucci, 1983; Zeebe and Wolf-
44 Gladrow, 2001). The saturation state of CaCO_3 (Ω_{CaCO_3}) is calculated with seawater
45 concentrations of Ca^{2+} and CO_3^{2-} and K_{sp}^* as:

46

$$47 \quad \Omega_{\text{CaCO}_3} = \frac{[\text{Ca}^{2+}]_{\text{seawater}} [\text{CO}_3^{2-}]_{\text{seawater}}}{K_{\text{sp}}^*} \quad (3)$$

48 Accordingly, CaCO_3 precipitation is thermodynamically favored when the product of
49 $[\text{Ca}^{2+}]_{\text{seawater}}$ and $[\text{CO}_3^{2-}]_{\text{seawater}}$ reaches or exceeds K_{sp}^* or $\Omega_{\text{CaCO}_3} \geq 1$. In the oceans, Ω_{CaCO_3} is
50 largely determined by $[\text{CO}_3^{2-}]$ because $[\text{Ca}^{2+}]$ is rather constant in seawater (Kleypas et al.,
51 1999).

52 Biogenic CaCO_3 is mainly present as calcite or aragonite, which have different crystal
53 structures and solubility. Calcite is predominantly formed by coccolithophores, foraminifera,
54 and some crustaceans while aragonite is typically found in scleractinian corals. Molluscs can
55 have both calcite and aragonite. Echinoderms and octocorals build calcite with a large fraction
56 of magnesium (Mg) included in the crystal lattice (Mann, 2001). Aragonite is more soluble

57 than calcite which is expressed in an offset between their individual K_{sp}^* values (Mucci,
58 1983). This offset, however, is the only major difference in their solubility and changes in
59 $\Omega_{\text{aragonite}}$ are very similar to changes in Ω_{calcite} (Zeebe and Wolf-Gladrow, 2001). They are
60 therefore summarized in the term Ω_{CaCO_3} in this study since changes in the saturation state
61 rather than absolute numbers are addressed here.

62 On the biological level, chemical precipitation of CaCO_3 as defined in Eq. (1) is just the final
63 step in the calcification process. Before precipitation, calcium and inorganic carbon have to be
64 transported in a series of active and/or passive processes until they reach the site of
65 calcification which is usually located in specialized cellular compartments, tissues, or tissue
66 interfaces. Transport mechanisms and pathways are highly diverse among the various
67 calcifying taxa which rules out the possibility to formulate a generally applicable calcification
68 model (Mann, 2001). What all calcifiers have in common, however, is their dependency on
69 calcium and inorganic carbon availability in seawater as this is the ultimate source medium
70 (Weiner and Addadi, 2011). Thus, biotic calcification will respond to changes in seawater
71 calcium and inorganic carbon when concentrations cross species-specific thresholds.

72 Calcium is present in seawater in high concentrations ($\sim 10 \text{ mmol kg}^{-1}$) as Ca^{2+} (Zeebe and
73 Wolf-Gladrow, 2001). As this ion is also the form used in the final precipitation reaction (Eq.
74 (1)), calcium does not need to be chemically transformed while being transported from
75 seawater to the site of calcification (Allemand et al., 2004; Bentov et al., 2009; Mackinder et
76 al., 2011). This is in clear contrast to CO_3^{2-} where, the relation between ion source from
77 seawater and ion sink during crystallization is considerably more complex since CO_3^{2-} is in
78 constant exchange with HCO_3^- and CO_2 . Thus, CO_3^{2-} used for CaCO_3 crystallization (Eq. (1))
79 at the site of calcification does not have to be taken from the seawater CO_3^{2-} pool but could
80 equally well originate from the seawater CO_2 or HCO_3^- reservoir and be transformed to CO_3^{2-}
81 shortly before reacting with Ca^{2+} .

82 Despite the unknown seawater DIC source for CaCO_3 precipitation, $[\text{CO}_3^{2-}]$ or the CO_3^{2-} -
83 dependent Ω_{CaCO_3} are often considered *a priori* as the key carbonate system parameters
84 determining calcification rates or the fitness of calcifying organisms in the oceans (Kleypas et
85 al., 1999; Beaufort et al., 2011). This assumption is reasonable under corrosive conditions (i.e.
86 $\Omega_{\text{CaCO}_3} < 1$) where $[\text{CO}_3^{2-}]$ controls the dissolution of CaCO_3 (Eq. (3)). The relevance of
87 $[\text{CO}_3^{2-}]$ for the formation of CaCO_3 is, however, poorly constrained because very little is
88 known about a molecular uptake and transport system that can take CO_3^{2-} from seawater and

89 transfer it to the site of calcification. This uncertainty leads to the key questions: Which
90 inorganic carbon species in seawater is/are utilized and which other carbonate system
91 parameter(s) could be relevant for calcification?

92 Several physiological studies with different calcifying taxa have addressed these questions by
93 setting up experiments where the influence of individual carbonate system parameters could
94 be studied in isolation. Some of these studies found the best correlations of calcification rates
95 with $[CO_3^{2-}]$ and Ω_{CaCO_3} (e.g. Schneider and Erez, 2006; Gazeau et al., 2011; de Putron et al.,
96 2011; Keul et al., 2013; Waldbusser et al., 2014) while others highlighted the importance of
97 $[HCO_3^-]$ (e.g. Buitenhuis et al., 1999; Jury et al., 2010). Still others found that the response is
98 not controlled by a single carbonate system parameter but the interplay of two or more. In
99 coccolithophores, for example, calcification rates were repeatedly shown to increase from low
100 to intermediate DIC but decrease again above certain thresholds (Langer et al., 2006; Bach et
101 al., 2011; 2015; Sett et al., 2014). This optimum-curve response pattern was explained by the
102 interaction between HCO_3^- and protons (H^+) where HCO_3^- stimulates calcification as substrate
103 and H^+ functions as inhibitor (Bach et al., 2011, 2013). Similar conclusions have also been
104 made in studies with bivalves (Thomsen et al., 2015) and corals (Jury et al., 2010) where it
105 has been noted that the calcification response to changing carbonate chemistry could be the
106 result of the opposing effects of $[HCO_3^-]$ and $[H^+]$.

107 Jokiel (2011a, 2011b, 2013) went one step further. Based on the results of his work on coral
108 reef calcification he argued that single carbonate chemistry parameters such as $[CO_3^{2-}]$ or
109 Ω_{CaCO_3} have no basic physiological meaning for calcification. Instead, calcification is
110 controlled by the interaction of a “reactant” (i.e. DIC) and an “inhibitor” (i.e. H^+) and that
111 calcification rates only correlate with $[CO_3^{2-}]$ because $[CO_3^{2-}]$ itself is linearly correlated with
112 the ratio of reactant to inhibitor (i.e. DIC/ $[H^+]$) (Jokiel, 2013; Jokiel et al., 2014).

113 The present study builds up on these previous findings and aims to refine the thought that
114 calcification is not controlled by a single carbonate chemistry parameter but reacts to a
115 combination of two or more. Therefore, attention will be drawn to a potentially important
116 proportionality between $[CO_3^{2-}]$, or Ω_{CaCO_3} , and the $[HCO_3^-]/[H^+]$ ratio which was uncovered
117 by rearranging carbonate chemistry equations. I will discuss (1) how this proportionality
118 could help to understand carbonate chemistry induced changes in $CaCO_3$ precipitation by
119 marine organisms; (2) how this proportionality could modify the paradigm that high latitude
120 calcifiers are more susceptible to ocean acidification than species living in low latitudes.

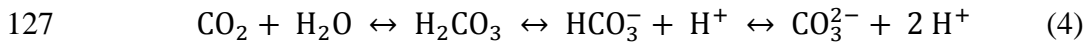
121

122 **2 Material and Methods**

123 **2.1 Uncovering the proportionality between $[\text{CO}_3^{2-}]$, or Ω_{CaCO_3} , and the $[\text{HCO}_3^-]/[\text{H}^+]$ ratio**

125 The carbonate system is an equilibrium reaction of the form:

126



128

129 which can be simplified to:

130



132

133 because $[\text{H}_2\text{CO}_3]$ is only about 1/1000 of $[\text{CO}_2]$ and has no special significance to the acid-
134 base equilibria since both species are uncharged (Butler, 1998; Dickson 2010). Hence, $[\text{CO}_2]$
135 is summarized in the following as:

136

137 $[\text{CO}_2] = [\text{CO}_2]_{\text{aq}} + [\text{H}_2\text{CO}_3]$ (6)

138

139 where aq denotes for gaseous CO_2 dissolved in seawater.

140 For the description of the carbonate system, the first and second dissociation constants (K_1
141 and K_2) are expressed in terms of concentrations - i.e. as stoichiometric dissociation
142 constants:

143

144 $K_1^* = \frac{[\text{HCO}_3^-][\text{H}^+]}{[\text{CO}_2]}$ (7)

145

146 and

147

148

$$K_2^* = \frac{[CO_3^{2-}][H^+]}{[HCO_3^-]} \quad (8)$$

149

150 which are a function of temperature, salinity, and pressure (Zeebe and Wolf-Gladrow, 2001).
151 Solving Eq. (8) for $[HCO_3^-]/[H^+]$ as:

152

153

$$\frac{[HCO_3^-]}{[H^+]} = \frac{1}{K_2^*} [CO_3^{2-}] \quad (9)$$

154

155 shows that $[CO_3^{2-}]$ is proportional to $[HCO_3^-]/[H^+]$ when temperature, salinity, and pressure
156 remain unchanged because K_2^* is constant under these circumstances.

157 The $CaCO_3$ saturation state of seawater has been defined in Eq. (3). Solving Eq. (3) and Eq.
158 (9) for $[CO_3^{2-}]$ yields:

159

160

$$[CO_3^{2-}] = \frac{\Omega_{CaCO_3} K_{sp}^*}{[Ca^{2+}]} \quad (10)$$

161

162 and

163

$$[CO_3^{2-}] = \frac{[HCO_3^-]K_2^*}{[H^+]} \quad (11)$$

164

165 Combining these equations and subsequently solving them for $[HCO_3^-]/[H^+]$ yields:

166

167

$$\frac{[HCO_3^-]}{[H^+]} = \frac{\Omega_{CaCO_3} K_{sp}^*}{[Ca^{2+}] K_2^*} \quad (12)$$

168

169 It follows that $[HCO_3^-]/[H^+]$ and Ω_{CaCO_3} are proportional, under constant T, S, and P. Note
170 that $[Ca^{2+}]$ is conservative in seawater and therefore scales with salinity.

171

172 **2.2 Carbonate chemistry calculations**

173 Carbonate chemistry data presented in Figs. 1-7 were calculated with the MATLAB (the
174 Mathworks) version of CO2SYS (van Heuven et al., 2011) using K_1^* and K_2^* determined by
175 (Millero, 2010), K_{HSO_4} by Dickson (1990), and K_{sp}^* determined by Mucci (1983). $[\text{H}^+]$ (free
176 scale) was subsequently calculated from pH_{free} :

177

178
$$\text{pH}_{\text{free}} = -\log[\text{H}^+]_{\text{free}} \quad (13)$$

179

180 as given in (Zeebe and Wolf-Gladrow, 2001).

181 Surface ocean (0-50 m) carbonate chemistry (DIC, TA), nutrient (PO_4^{3-}), salinity, and
182 temperature data used for calculations presented in Figs. 1, 5B, D, F, and 6 were extracted
183 from a model simulation with the University of Victoria (UVic) Earth System model
184 performed by Taucher and Oschlies (2011). In their study, the model was spun up for 4000
185 years with pre-industrial boundary conditions and then forced with reconstructed CO_2
186 emissions and aerosol dynamics for the period from 1765-2000 (Schmittner et al., 2008).
187 Thereafter, the model was forced with anthropogenic CO_2 emissions as predicted in the IPCC
188 A2 ("business-as-usual") scenario. Note that the data was taken from their reference run
189 ("TEMP"). For further details on the model setup, please refer to the original description by
190 Taucher and Oschlies (2011).

191 The ratios $[\text{CO}_3^{2-}]$ / $([\text{HCO}_3^-]/[\text{H}^+])$ and $[\text{CO}_3^{2-}]$ / $(\text{DIC}/[\text{H}^+])$ shown in Fig. 3 were calculated
192 with CO2SYS assuming increasing pCO_2 at constant total alkalinity ($2350 \mu\text{mol kg}^{-1}$),
193 phosphate and silicate concentrations to be zero, and T, S, and P of 15°C , 35, and 0 dbar,
194 respectively.

195 Sensitivities of $[\text{CO}_3^{2-}]$, Ω_{CaCO_3} , and $[\text{HCO}_3^-]/[\text{H}^+]$ to changing P, S, or T (Fig. 4) were
196 calculated with CO2SYS assuming phosphate and silicate concentrations to be zero, a
197 constant pCO_2 of $400 \mu\text{atm}$, and a constant TA of $\sim 2350 \mu\text{mol kg}^{-1}$. The parameters that were
198 not varied within the particular calculation were set to constant values of 15°C , 35, and 0 dbar
199 for T, S, and P, respectively.

200 Calcification related measurements and corresponding DIC, TA, T, S, and nutrient data of
201 experiments with different species (Schneider and Erez, 2006; Gazeau et al., 2011; Keul et al.,
202 2013, Fig. 2) were downloaded from the PANGAEA data server (www.pangaea.de).

203 Surface ocean (0 - 100 m) carbonate chemistry, physical, and nutrient data of the meridional
204 Atlantic transect measured during CLIVAR cruises in 2003 (Peltola et al., 2003) and 2005
205 (Wanninkhof et al., 2006) (Fig. 5A, C, E) were downloaded from the CARINA data synthesis
206 homepage (<http://cdiac.ornl.gov/oceans/CARINA/>). Water-column carbonate chemistry,
207 physical, and nutrient data between 1988 and 2012 from the ALOHA time-series station (Fig.
208 7) in the central Pacific (22° 45' N 158° 00' W) were downloaded from the ALOHA website
209 (<http://aco-ssds.soest.hawaii.edu/ALOHA/>).

210

211 **3 Results and discussion**

212 **3.1 Is HCO_3^- or CO_3^{2-} the more suitable inorganic carbon substrate for 213 calcification?**

214 It is important to determine the calcification-relevant inorganic carbon species taken from
215 seawater in order to understand the calcification response of marine organisms to changing
216 carbonate chemistry. Most studies assume that HCO_3^- rather than CO_3^{2-} is the key inorganic
217 carbon ion (e.g. Allemand et al., 2004; Mackinder et al., 2010; Stumpp et al., 2012; Taylor et
218 al., 2012). However, proof of this assumption on a physiological level is still missing because
219 attempts to unequivocally determine the inorganic carbon molecule transported by molecular
220 transport systems were not successful so far (Pushkin and Kurtz, 2006; Mackinder et al.,
221 2010; Lee et al., 2013; Romero et al., 2013). Furthermore, the uptake mechanisms for
222 inorganic carbon are highly diverse among the various calcifying taxa so that generalization
223 of physiological principles would be difficult (see section 3.6 for a discussion on this topic). It
224 may therefore be helpful to approach this question differently and ask more generally whether
225 HCO_3^- or CO_3^{2-} would be the more suitable inorganic carbon substrate for calcification. Three
226 different perspectives will be addressed in the following.

227 **3.1.1 Abundance**

228 HCO_3^- is usually the most abundant DIC species in seawater. At pH_f (free scale) of 8.1 it
229 contributes ~90% to the total DIC pool while CO_3^{2-} contributes less than 10%. Thus,
230 molecular CO_3^{2-} transporters would require a nine times higher affinity to their substrate than

231 HCO_3^- transporters. It may therefore make more sense for an organism to rely on the largest
232 inorganic carbon pool if molecular transporters take the ions directly from seawater
233 (Mackinder et al., 2010).

234 **3.1.2 Homeostasis**

235 The hydration timescale of CO_2 ($\text{CO}_2 + \text{H}_2\text{O} \leftrightarrow \text{HCO}_3^- + \text{H}^+$) is comparatively slow (~ 10 seconds), while the hydrolysis of HCO_3^- ($\text{HCO}_3^- \leftrightarrow \text{CO}_3^{2-} + \text{H}^+$) is fast ($\sim 10^{-7}$ seconds; Zeebe and Wolf-Gladrow, 2001; Schulz et al., 2006). Assuming a transcellular pathway, selectively
236 incorporated CO_3^{2-} that is transported through cytosol with a typical pH around $\sim 7.0 - 7.4$
237 (Madshus, 1988) would quickly turn into HCO_3^- unless the transfer is faster than 10^{-7} seconds.
238 In the likely case that the transfer takes longer, CO_3^{2-} would bind a proton in the cytosol and
239 be transported as HCO_3^- to the site of calcification where the proton would subsequently be
240 released back to the cytosol during CaCO_3 precipitation. Hence, the cytosolic pH would
241 remain stable in case of selective CO_3^{2-} uptake as long as CO_3^{2-} uptake and CaCO_3
242 precipitation occur at the same rate. However, both processes may occasionally run out of
243 equilibrium for short periods. In these cases, the utilization of CO_3^{2-} as inorganic carbon
244 source would constitute a substantial risk for the organisms' pH homeostasis. Excess CO_3^{2-}
245 uptake would elevate cytosolic pH while excess CaCO_3 precipitation would reduce it. In
246 contrast, a selective uptake of HCO_3^- from seawater would perturb the cytosolic pH to a much
247 smaller extent when HCO_3^- uptake and CaCO_3 precipitation are not entirely balanced because
248 HCO_3^- has a relatively low potential to accept or donate H^+ at a typical pH of 7.2. It may
249 therefore be easier for calcifiers to keep cytosolic pH stable at ~ 7.2 when using HCO_3^- .
250

252 **3.1.3 Stability**

253 Seawater carbonate chemistry conditions are relatively stable on longer timescales but can
254 fluctuate substantially on a seasonal and diurnal cycle (Takahashi et al., 1993; Thomsen et al.,
255 2010; Shaw et al., 2013), especially in diffusive boundary layers of organisms (Wolf-Gladrow
256 and Riebesell, 1997; Flynn et al., 2012; Glas et al., 2012a; Agostini et al., 2013). Fluctuations
257 are mostly induced by photosynthetic or respiratory turnover of CO_2 . The magnitude of
258 fluctuation scales with the productivity of the ecosystem (Schulz and Riebesell, 2013) but
259 fluctuations should usually stay within the $\sim 6.5 - 9$ pH range. HCO_3^- is dominant and has a
260 relatively stable concentration in this entire pH range, while $[\text{CO}_3^{2-}]$ is highly variable. In the
261 habitat of a temperate coraline algae, for example, typical diurnal pH fluctuations can range

262 from ~8.4 at day to ~7.6 at night (Cornwall et al., 2013). These changes would translate in a
263 moderate day/night difference of ~30% in $[HCO_3^-]$ but a pronounced difference of more than
264 450% in $[CO_3^{2-}]$. Hence, HCO_3^- is the much more reliable inorganic carbon source for
265 calcification as it shows significantly smaller variability.

266 **3.2 Relationship between calcification and $[CO_3^{2-}]$ or $[HCO_3^-]/[H^+]$ in existing
267 datasets**

268 If the common assumption holds and marine calcifiers primarily utilize HCO_3^- instead of
269 CO_3^{2-} as $CaCO_3$ substrate (see previous section) then correlations between calcification and
270 $[CO_3^{2-}]$ or Ω_{CaCO_3} are not useful under non-corrosive conditions. Still, these correlations often
271 yield high coefficients of determination (R^2) even if conditions are super-saturated (Schneider
272 and Erez, 2006; Marubini et al., 2008; de Putron et al., 2011; Gazeau et al., 2011; Keul et al.,
273 2013; Waldbusser et al., 2014). This dilemma can be resolved when considering the
274 proportionality between $[CO_3^{2-}]$, Ω_{CaCO_3} , and $[HCO_3^-]/[H^+]$ derived above. Every correlation
275 between calcification and $[CO_3^{2-}]$ or Ω_{CaCO_3} will be identical to the corresponding correlation
276 with $[HCO_3^-]/[H^+]$ when T, S, and P are stable (see Eqs. (9), (12)).

277 This is illustrated with data from three publications where the influence different carbonate
278 chemistry parameters on calcification rates was disentangled (Schneider and Erez, 2006;
279 Gazeau et al., 2011; Keul et al., 2013) (Fig. 2). All three studies conclude that $[CO_3^{2-}]$
280 determines calcification rates although calcification rates or calcification related
281 measurements of the hermatypic coral *Acropora eurystoma* (Schneider and Erez, 2006), the
282 benthic foraminifer *Ammonia* spec. (Keul et al., 2013), and larvae of the Pacific oyster
283 *Crassostrea gigas* (Gazeau et al., 2011) correlate equally well to $[HCO_3^-]/[H^+]$.

284 **3.3 Conceptual basis for the calcification control of $[HCO_3^-]/[H^+]$**

285 Implicit in the $[HCO_3^-]/[H^+]$ ratio is the thought that biotic $CaCO_3$ precipitation is balanced by
286 the stimulating influence of an inorganic carbon substrate and the negative influence of an
287 inhibitor (Bach et al., 2011; 2013; 2015; Jokiel, 2011a, 2011b, 2013; Jokiel et al., 2014).
288 Higher $[HCO_3^-]$ would stimulate calcification rates as a substrate whereas high seawater $[H^+]$
289 would inhibit them.

290 When both, $[HCO_3^-]$ and $[H^+]$ increase, calcification would be balanced by the degree of
291 change of these two ions. $[H^+]$ increases profoundly under ocean acidification while $[HCO_3^-]$
292 increases only marginally (Fig. 1, see also Schulz et al., 2009). Here, changing $[H^+]$ should be

293 of dominant control (Bach et al., 2011). When increasing $[H^+]$ is paralleled by a significant
294 increase of $[HCO_3^-]$, then the additional bicarbonate could potentially compensate the
295 inhibitory proton effect to some extent (Bach et al. 2015). Indeed, HCO_3^- uptake is a common
296 mechanism to buffer acidosis and might be facilitated at higher HCO_3^- availability (Boron,
297 2004; Melzner et al., 2009; Stumpp et al., 2012).

298 The inhibition by high seawater $[H^+]$ is tightly linked to the production of $CaCO_3$ from Ca^{2+}
299 and HCO_3^- because calcification is then a source of H^+ ($Ca^{2+} + HCO_3^- \rightarrow CaCO_3 + H^+$). H^+
300 generated that way would subsequently have to be released back into seawater to avoid
301 acidification at the site of calcification. This removal should be relatively easy when seawater
302 $[H^+]$ is low (i.e. pH is high). It could become more difficult, however, when seawater $[H^+]$
303 rises and the inside-out $[H^+]$ gradient shrinks (Cyronak et al., 2015; Jokiel, 2011b; Taylor et
304 al., 2011; Stumpp et al., 2012; Venn et al., 2013).

305 3.4 Similarities and differences between the $DIC/[H^+]$ and the $[HCO_3^-]/[H^+]$ ratio

306 In a series of papers Jokiel (2011a, 2011b, 2013) proposed that carbonate chemistry controls
307 calcification rates in corals through the combined influence of DIC (“reactant”) and H^+
308 (“inhibitor”) and noted that favorable carbonate chemistry conditions are established when the
309 ratio of DIC to $[H^+]$ is high. Hence, the underlying thought implicit in the $DIC/[H^+]$ ratio is
310 identical to that implemented in the “substrate-inhibitor-ratio” defined here as $[HCO_3^-]/[H^+]$.

311 Jokiel (2011a, 2011b, 2013) also noted that there is a linear correlation between $DIC/[H^+]$ and
312 $[CO_3^{2-}]$. The correlation observed by Jokiel exists because the DIC pool is dominated by
313 HCO_3^- ions under normal pH conditions (see section 3.1.1) and therefore typically follows the
314 same rules as the proportionality between $[HCO_3^-]/[H^+]$ and $[CO_3^{2-}]$ uncovered in section 2.1.
315 However, when the fraction of HCO_3^- in the DIC pool declines, the $DIC/[H^+]$ vs. $[CO_3^{2-}]$
316 correlation starts to increasingly deviate from linearity. In the oceans, noticeable deviations
317 start in the pCO_2 range below 250-500 μ atm, where an exponentially increasing fraction of
318 the DIC pool is present as CO_3^{2-} (Fig. 3). Thus, exchanging $DIC/[H^+]$ with $[CO_3^{2-}]$ to explain
319 the calcification response to carbonate chemistry (comparable to what has been done in Fig.
320 2) is not meaningful when pCO_2 is below this range. This problem does not exist for the
321 $[HCO_3^-]/[H^+]$ ratio where the linear relation holds under all carbonate chemistry conditions as
322 long as T, S, and P are constant (Fig. 3).

323 Whether the $DIC/[H^+]$ ratio proposed by Jokiel (2011a, 2011b, 2013) or the $[HCO_3^-]/[H^+]$
324 ratio could be the more meaningful parameter to explain the carbonate chemistry response of

325 calcification depends on the investigated organism. The DIC/[H⁺] ratio would be more
326 meaningful if the organism takes up all DIC species in the same proportion as present in
327 seawater while the [HCO₃⁻]/[H⁺] ratio would be more appropriate when selective uptake on
328 HCO₃⁻ occurs (see also section 3.6.4).

329 **3.5 Global implications**

330 The following paragraphs will address to what extent our view on carbonate chemistry control
331 of calcification in the oceans could be modified when we consider [HCO₃⁻]/[H⁺] rather than
332 [CO₃²⁻] or Ω_{CaCO_3} as the most influential parameter. Before starting the discussion I would
333 like to emphasize, however, that carbonate chemistry patterns discussed here are just one
334 among other abiotic (e.g. temperature or light) or biotic (e.g. food availability or competition)
335 factors which must also be taken into consideration when trying to understand the patterns of
336 calcification in the oceans.

337 **3.5.1 Latitudinal and vertical gradients in [HCO₃⁻]/[H⁺], [CO₃²⁻], and Ω_{CaCO_3}**

338 The proportionality between [CO₃²⁻], Ω_{CaCO_3} , and [HCO₃⁻]/[H⁺] derived in section 2.1 is only
339 valid as long temperature, salinity, and pressure are constant and do not alter K₂^{*} and K_{sp}^{*}. If
340 these parameters change, then the proportionality no longer holds and the response of
341 calcification would be different, depending on whether calcifiers react to [CO₃²⁻], Ω_{CaCO_3} , or
342 [HCO₃⁻]/[H⁺].

343 The influence of temperature, salinity, and pressure is illustrated in Fig. 4. Increasing pressure
344 has a negative effect on all three carbonate system components. It is most pronounced on
345 Ω_{CaCO_3} and weakest on [CO₃²⁻] (Fig. 4A). Increasing salinity has a positive influence on
346 [CO₃²⁻] and Ω_{CaCO_3} but a negative one on [HCO₃⁻]/[H⁺] (Fig. 4B). Its influence, however, is
347 low since salinity gradients in the oceans are generally too weak to be of high relevance in
348 this context. Increasing temperature has a profound positive impact on [CO₃²⁻] and Ω_{CaCO_3} but
349 almost no influence on [HCO₃⁻]/[H⁺] (Fig. 4C).

350 In combination, these factors cause a highly interesting difference of [CO₃²⁻], Ω_{CaCO_3} , and
351 [HCO₃⁻]/[H⁺] on a latitudinal gradient. While Ω_{CaCO_3} and [CO₃²⁻] decrease 2-3 fold towards
352 the poles, [HCO₃⁻]/[H⁺] is almost constant over the same range (Figs. 5, 6). This inconsistency
353 is mostly due to different temperature sensitivities among the three parameters. Cooler
354 temperatures in high latitudes lead to higher solubility of CO₂ which results in an equilibrium
355 shift away from [CO₃²⁻] towards [CO₂] and [HCO₃⁻] (Eq.(4)). Accordingly, [CO₃²⁻] declines

356 towards the poles. Ω_{CaCO_3} follows the concentration of CO_3^{2-} since $[\text{Ca}^{2+}]$ is too stable to be of
357 any relevance. The slight poleward increase of $[\text{HCO}_3^-]$ is balanced by the concomitant
358 increase in $[\text{H}^+]$ which explains the stability of $[\text{HCO}_3^-]/[\text{H}^+]$ over the latitudinal gradient.
359 Thus, carbonate chemistry conditions for biotic CaCO_3 production would be fairly constant
360 over the entire surface ocean if controlled by $[\text{HCO}_3^-]/[\text{H}^+]$, whereas they would show a
361 profound poleward deterioration if determined by $[\text{CO}_3^{2-}]$ or Ω_{CaCO_3} (Figs. 5, 6).

362 Vertically, $[\text{CO}_3^{2-}]$ and Ω_{CaCO_3} decrease more severely than $[\text{HCO}_3^-]/[\text{H}^+]$ from surface to
363 about a thousand meters depth (~5-fold vs. ~3-fold decrease, Fig. 7). This has two reasons.
364 First, the temperature decline, which is strongest in the upper few hundred meters, negatively
365 affects $[\text{CO}_3^{2-}]$ and Ω_{CaCO_3} whereas $[\text{HCO}_3^-]/[\text{H}^+]$ remains unaffected (Fig. 4C). Second, the
366 increase of $[\text{H}^+]$ from 0-1000 m due to respiratory CO_2 release is paralleled by ~30%
367 increases of $[\text{HCO}_3^-]$ which mitigates the decline of $[\text{HCO}_3^-]/[\text{H}^+]$. Below a thousand meters,
368 all three carbonate system parameters are relatively stable. Of the three carbonate system
369 parameters considered here, $[\text{HCO}_3^-]/[\text{H}^+]$ is the most homogeneous when comparing the
370 development over the entire water column. Thus, the deterioration of carbonate chemistry
371 conditions for biotic CaCO_3 formation with depth would be less pronounced if it was
372 controlled by $[\text{HCO}_3^-]/[\text{H}^+]$ (Fig. 7).

373 **3.5.2 Implications for ocean acidification research**

374 The ongoing perturbation of the surface ocean by anthropogenic CO_2 causes a decline of
375 Ω_{CaCO_3} , $[\text{CO}_3^{2-}]$, and $[\text{HCO}_3^-]/[\text{H}^+]$. The magnitude of change in all three parameters is very
376 similar to each other on global average (Fig. 1). Until 2100 they decrease to about half the
377 value in the year 2000 (Figs. 1, 5). The two different latitudinal patterns for Ω_{CaCO_3} , $[\text{CO}_3^{2-}]$,
378 or $[\text{HCO}_3^-]/[\text{H}^+]$ are, however, conserved in the course of climate change (Fig. 6). Hence,
379 latitudinal differences among the three parameters are prevailing for longer timescales and are
380 not restricted to the current status of the carbonate system.

381 The presence of two highly different latitudinal patterns has important implications for ocean
382 acidification research. Polar regions have been identified as the most severely acidification-
383 affected regions on Earth as they are the first to experience corrosive conditions (i.e. $\Omega_{\text{CaCO}_3} < 1$;
384 Orr et al., 2005; Fabry et al., 2009; Hofmann et al., 2010). The vulnerability of high
385 latitudes is therefore explained by an abiotic process - i.e. CaCO_3 dissolution. The study
386 presented here deals with controls on the opposite process - i.e. biotic CaCO_3 formation.
387 Dissolution is determined by Ω_{CaCO_3} and there is no doubt that polar regions are most severely

388 affected (see also Fig. 6). From the production perspective, however, this is not necessarily
389 the case. Ocean acidification would be equally harmful in warm-water habitats as in the polar
390 realm in case CaCO_3 formation is controlled by $[\text{HCO}_3^-]/[\text{H}^+]$ and not $[\text{CO}_3^{2-}]$ or Ω_{CaCO_3} .
391 Thus, when high latitude organisms find a way to efficiently protect their crystal skeletons
392 from corrosive seawater, then they may not be more vulnerable to ocean acidification than
393 their warm water counterparts.

394 **3.6 Limitations and uncertainties**

395 This study has argued that a substrate-inhibitor ratio like $[\text{HCO}_3^-]/[\text{H}^+]$ (or $\text{DIC}/[\text{H}^+]$; Jokiel
396 2011a, 2011b, 2013) could be a useful measure to assess which carbonate chemistry
397 conditions could be favorable for calcification. However, it must also be recognized that such
398 a rather general view on carbonate chemistry control of calcification has its limitations when
399 it comes to a more detailed physiological level. Calcification follows an enormous variety of
400 pathways among the different taxa, with distinct inorganic carbon uptake mechanisms, and
401 distinct sensitivities to H^+ . Thus, the capability of the substrate-inhibitor ratio to predict
402 calcification rates can always be confounded by taxon-specific physiological features. The
403 most important limitations and uncertainties for the ability of $[\text{HCO}_3^-]/[\text{H}^+]$ to serve as
404 predictor variable for the carbonate chemistry control of calcification will be discussed in the
405 following.

406 **3.6.1 Corrosive conditions - accounting for the difference between gross and 407 net calcification**

408 When discussing the influence of carbonate chemistry on calcification, distinction needs to be
409 made between formation and dissolution of CaCO_3 since these two processes are possibly
410 controlled by different carbonate chemistry parameters. The roles of CaCO_3 formation and
411 dissolution are incorporated into the terms gross and net calcification. The former exclusively
412 refers to the precipitation of CaCO_3 whereas the latter accounts for both precipitation and
413 dissolution. The ratio of $[\text{HCO}_3^-]$ and $[\text{H}^+]$ can potentially be very useful to determine gross
414 calcification which equals net calcification under non-corrosive conditions (i.e. $\Omega_{\text{CaCO}_3} > 1$).
415 When Ω_{CaCO_3} falls below 1, however, the control of $[\text{HCO}_3^-]/[\text{H}^+]$ on gross calcification would
416 be obscured by the abiotic influence of Ω_{CaCO_3} on dissolution. Accordingly, corrosive
417 conditions would require consideration of both $[\text{HCO}_3^-]/[\text{H}^+]$ and Ω_{CaCO_3} in order to correctly
418 estimate the impact of carbonate chemistry on net biotic CaCO_3 formation.

419 Areas with corrosive conditions will expand under ocean acidification (Orr et al., 2005) so
420 that CaCO_3 dissolution becomes more widespread problem for future calcifiers. However,
421 dealing with dissolution of CaCO_3 is only of secondary relevance for living organisms as
422 everything that dissolves needs to be formed in the first place. Hence, although dissolution
423 processes cannot be left unconsidered, it is reasonable from a biological point of view to focus
424 on the processes that control formation of CaCO_3 .

425 **3.6.2 Applicability of $[\text{HCO}_3^-]/[\text{H}^+]$ in the geological record**

426 The restriction of $[\text{HCO}_3^-]/[\text{H}^+]$ to gross calcification rates (see previous section) limits its
427 applicability in the geological record because the information on CaCO_3 accumulation
428 conserved in the sediments is not only affected by gross calcification but also by post-
429 production dissolution and abiotic modifications of CaCO_3 during diagenesis which are both
430 controlled by Ω_{CaCO_3} . Thus, in order to verify the substrate-inhibitor concept for the
431 geological record we would need a reliable proxy for exclusively biotic gross calcification.
432 Conversely, the application of Ω_{CaCO_3} to explain trends in CaCO_3 sedimentation (e.g. Hönisch
433 et al., 2012; Ridgwell, 2005) would be reasonable because sedimentation involves both
434 precipitation and dissolution and Ω_{CaCO_3} is a good indicator for the former (under constant T,
435 S, P) and the key parameter for the latter.

436 **3.6.3 Extreme concentrations of HCO_3^- and H^+**

437 In some studies, calcification rates correlated better with $[\text{HCO}_3^-]$ than with $[\text{CO}_3^{2-}]$ (and thus
438 $[\text{HCO}_3^-]/[\text{H}^+]$) (Bach et al., 2013; Jury et al., 2010), which challenges the potential of $[\text{HCO}_3^-]$
439 $]/[\text{H}^+]$ to serve as predictor variable for CaCO_3 production. However, the dominant control of
440 HCO_3^- in these particular studies can be easily understood when considering the low HCO_3^-
441 concentrations at which its dominance actually occurred. The influence of $[\text{HCO}_3^-]$ relative to
442 $[\text{H}^+]$ will become more and more influential under conditions where HCO_3^- becomes
443 increasingly limiting. Conversely, any influence of $[\text{HCO}_3^-]$ will become negligible when the
444 organism is fully saturated with it. Under these circumstances calcification is most likely
445 primarily controlled by $[\text{H}^+]$ (Bach et al., 2011; Jokiel 2011b; Taylor et al., 2011). Thus, the
446 potential of $[\text{HCO}_3^-]/[\text{H}^+]$ in predicting calcification is low at rather 'extreme' carbonate
447 chemistry conditions where the influence of either HCO_3^- or H^+ strongly outweighs the other.
448 Its potential should be high, however, under conditions where the investigated organism is
449 responsive to both $[\text{HCO}_3^-]$ and $[\text{H}^+]$.

450 **3.6.4 Transport of seawater**

451 Some foraminifera and coral species have been reported to transfer calcification-relevant ions
452 to the site of CaCO_3 precipitation by means of seawater transport (Bentov et al., 2009; de
453 Nooijer et al., 2009; Gagnon et al., 2012; Tambutté et al., 2012). In the case of foraminifera,
454 seawater is engulfed in membrane vesicles, transported to the site of calcification, and on its
455 way alkalized to increase $[\text{CO}_3^{2-}]$ (Bentov et al., 2009; de Nooijer et al., 2009). In the case of
456 corals, seawater (or at least its constituents smaller than 20 nm; Tambutté et al., 2012) may
457 pass epithelia and reach the CaCO_3 skeleton via the paracellular pathway. For both processes
458 (seawater endocytosis and seawater leakage along the intercellular space), all DIC species are
459 potential inorganic carbon sources to fuel calcification. Hence, for organisms which purely
460 rely on seawater endocytosis/leakage, the $\text{DIC}:[\text{H}^+]$ ratio proposed by Jokiel (2011a, 2011b,
461 2013) could be more appropriate to explain the calcification response to carbonate chemistry
462 than $[\text{HCO}_3^-]/[\text{H}^+]$.

463 **3.6.5 CO_2 as inorganic carbon source for calcification**

464 Some organisms receive significant amounts of inorganic carbon used for calcification from
465 respiratory sources (Pearse, 1970; Erez, 1978; Sikes et al., 1981; Tanaka et al., 1986; Furla et
466 al., 2000). Here, organisms do not exclusively rely on direct inorganic carbon utilization from
467 seawater but supplement calcification to a variable degree with CO_2 gained intracellularly
468 from respired biomass. This CO_2 utilization may be further strengthened (1) when metabolic
469 CO_2 is ‘trapped’ inside the organisms through the establishment of pH gradients which limit
470 the diffusive loss of CO_2 (Bentov et al., 2009, Glas et al., 2012b) or (2) when CO_2 is
471 transported actively towards the site of calcification (de Nooijer et al., 2014). Thus, CO_2
472 reacting with H_2O to form HCO_3^- and H^+ (catalyzed by the ubiquitous enzyme carbonic
473 anhydrase) could be an alternative inorganic carbon source for calcification in particular taxa.
474 The potential control of seawater $[\text{HCO}_3^-]/[\text{H}^+]$ on CaCO_3 precipitation may therefore be
475 weakened by the degree to which calcifiers utilize CO_2 as inorganic carbon source.

476 **3.6.6 Photoautotrophic calcifiers**

477 Photoautotrophic calcifiers such as coccolithophores or zooxanthellate corals not only
478 interact with HCO_3^- and H^+ but also with CO_2 . Photosynthetic and calcification-related
479 processes are physiologically coupled within photoautotrophs (Paasche, 2002; Allemand et
480 al., 2004). Accordingly, calcification rates will be affected indirectly when photosynthesis is

481 CO_2 limited (Bach et al., 2015). A valuable measure to determine the potential of CO_2 to limit
482 growth and photosynthesis is $K_{1/2}$ which denotes the CO_2 concentration where the process
483 runs at half of its maximum. Available $K_{1/2}$ measurements suggest that CO_2 limitation mostly
484 occurs well below CO_2 concentrations typically encountered by the organisms in their
485 respective habitats (Rost et al., 2003; Sett et al., 2014). Thus, its influence should rarely
486 interfere with the influence of $[\text{HCO}_3^-]/[\text{H}^+]$ under natural conditions.

487 **4 Conclusions**

488 A variety of studies highlighted that carbonate chemistry controls calcification through the
489 balance of stimulation by an inorganic carbon substrate (HCO_3^- or DIC) and inhibition by
490 protons (e.g. Bach et al., 2011; Jokiel 2011a; Thomsen et al., 2015). Other studies found that
491 $[\text{CO}_3^{2-}]$ or Ω_{CaCO_3} are the carbonate chemistry parameters which best predict calcification (e.g.
492 Schneider and Erez, 2006; de Putron et al., 2011; Gazeau et al., 2011; Waldbusser et al.,
493 2014). The proportionalities between $[\text{CO}_3^{2-}]$ or Ω_{CaCO_3} and the $[\text{HCO}_3^-]/[\text{H}^+]$ ratio derived in
494 Eqs. (9) and (12) provide the chemical basis to reconcile these conflicting results. Every
495 correlation between calcification and $[\text{CO}_3^{2-}]$ or Ω_{CaCO_3} will be identical to the corresponding
496 correlation with $[\text{HCO}_3^-]/[\text{H}^+]$ when T, S, and P are stable. Thus, the good correlations to
497 $[\text{CO}_3^{2-}]$ and Ω_{CaCO_3} that have previously been reported may have simply masked the combined
498 influence of $[\text{HCO}_3^-]$ and $[\text{H}^+]$ (see also findings by Jokiel, 2011a, 2011b, 2013; Jokiel et al.,
499 2014) which are arguably the physiologically more meaningful parameters to correlate gross
500 calcification with (Bach et al., 2013; Jokiel, 2013; Thomsen et al., 2015; section 3.1 and 3.3).

501 Accounting for the influence of $[\text{HCO}_3^-]/[\text{H}^+]$ in controlling CaCO_3 formation would also
502 have interesting implications for how we assess carbonate chemistry conditions and
503 calcification along a latitudinal gradient. A comparison of present and future $[\text{CO}_3^{2-}]$, Ω_{CaCO_3} ,
504 and $[\text{HCO}_3^-]/[\text{H}^+]$ patterns in the surface ocean revealed a strong poleward decline in $[\text{CO}_3^{2-}]$
505 and Ω_{CaCO_3} but no decline in $[\text{HCO}_3^-]/[\text{H}^+]$. These highly different latitudinal patterns are
506 conserved during climate change. Thus, it may turn out that ocean acidification is globally a
507 more uniform problem for biotic CaCO_3 formation than previously thought.

508

509 **Acknowledgements**

510 I thank Kai Schulz and Ulf Riebesell for our frequent discussions about carbonate chemistry
511 and calcification which led to the preparation of this manuscript. I am also grateful to Toste

512 Tanhua for support on CARINA data, Jan Taucher for sharing the UVic model output, as well
513 as Allanah Paul and Jan Taucher for proof-reading the manuscript. This study profited from
514 the motivating and constructive reviews by Lennart de Nooijer, Paul Jokiel, and two
515 anonymous reviewers. It was funded by the Federal Ministry of education and research
516 (BMBF) in the framework of the Biological Impacts of Ocean Acidification II (BIOACID II)
517 project (W.P. 1.3).

518

519 **References**

520 Agostini, S., Fujimura, H., Higuchi, T., Yuyama, I., Casareto, B. E., Suzuki, Y. and Nakano,
521 Y.: The effects of thermal and high-CO₂ stresses on the metabolism and surrounding
522 microenvironment of the coral *Galaxea fascicularis*., C. R. Biol., 336(8), 384–91,
523 doi:10.1016/j.crvi.2013.07.003, 2013.

524 Allemand, D., Ferrier-Pagès, C., Furla, P., Houlbrèque, F., Puverel, S., Reynaud, S.,
525 Tambutté, É., Tambutté, S. and Zoccola, D.: Biomineralisation in reef-building corals: from
526 molecular mechanisms to environmental control, Comptes Rendus Palevol, 3(6-7), 453–467,
527 doi:10.1016/j.crpv.2004.07.011, 2004.

528 Bach, L. T., Riebesell, U. and Schulz, K. G.: Distinguishing between the effects of ocean
529 acidification and ocean carbonation in the coccolithophore *Emiliania huxleyi*, Limnol.
530 Oceanogr., 56(6), 2040–2050, doi:10.4319/lo.2011.56.6.2040, 2011.

531 Bach, L. T., Mackinder, L. C. M., Schulz, K. G., Wheeler, G., Schroeder, D. C., Brownlee, C.
532 and Riebesell, U.: Dissecting the impact of CO₂ and pH on the mechanisms of photosynthesis
533 and calcification in the coccolithophore *Emiliania huxleyi*., New Phytol., 199(1), 121–34,
534 doi:10.1111/nph.12225, 2013.

535 Bach, L. T., Riebesell, U., Gutowska, M. A., Federwisch, L. and Schulz, K. G.: A unifying
536 concept of coccolithophore sensitivity to changing carbonate chemistry embedded in an
537 ecological framework, Prog. Oceanogr., 135, 125–138, doi:10.1016/j.pocean.2015.04.012,
538 2015.

539 Beaufort, L., Probert, I., de Garidel-Thoron, T., Bendif, E. M., Ruiz-Pino, D., Metzl, N.,
540 Goyet, C., Buchet, N., Coupel, P., Grelaud, M., Rost, B., Rickaby, R. E. M. and de Vargas,
541 C.: Sensitivity of coccolithophores to carbonate chemistry and ocean acidification., Nature,
542 476(7358), 80–83, doi:10.1038/nature10295, 2011.

543 Bentov, S., Brownlee, C. and Erez, J.: The role of seawater endocytosis in the
544 biomineralization process in calcareous foraminifera, Proc. Natl. Acad. Sci., 106(51), 21500–
545 21504, 2009.

546 Boron, W. F.: Regulation of intracellular pH, Adv. Physiol. Educ., 28, 160–179,
547 doi:10.1152/advan.00045.2004., 2004.

548 Buitenhuis, E. T., De Baar, H. J. W. and Veldhuis, M. J. W.: Photosynthesis and calcification
549 by *Emiliania huxleyi* (Prymnesiophyceae) as a function of inorganic carbon species, *J.*
550 *Phycol.*, 35(5), 949–959, 1999.

551 Butler, J. N.: Ionic equilibrium: solubility and pH calculations, John Wiley and sons, New
552 York., 1998.

553 Cornwall, C. E., Hepburn, C. D., McGraw, C. M., Currie, K. I., Pilditch, C. A., Hunter, K. A.,
554 Boyd, P. W. and Hurd, C. L.: Diurnal fluctuations in seawater pH influence the response of a
555 calcifying macroalga to ocean acidification, *Proc. R. Soc. B Biol. Sci.*, 280(1772), 2013.

556 Cyronak, T., Schulz, K. G. and Jokiel, P. L.: The Omega myth: what really drives lower
557 calcification rates in an acidifying ocean, *Ices J. Mar. Sci.*, doi:10.1093/icesjms/fsv075, 2015.

558 Dickson, A. G.: Standard potential of the reaction: $\text{AgCl}(\text{s}) + 12 \text{H}_2(\text{g}) = \text{Ag}(\text{s}) + \text{HCl}(\text{aq})$,
559 and the standard acidity constant of the ion HSO_4^- in synthetic sea water from 273.15 to
560 318.15 K, *J. Chem. Thermodyn.*, 22(2), 113–127, 1990.

561 Dickson, A. G.: The carbon dioxide system in seawater: equilibrium chemistry and
562 measurements, in Guide to best practices for ocean acidification research and data reporting,
563 edited by U. Riebesell, V. J. Fabry, L. Hansson, and J.-P. Gattuso, pp. 17–40, Publications
564 Office of the European Union, Luxembourg., 2010.

565 Erez, J.: Vital effect on stable-isotope composition seen in foraminifera and coral skeletons,
566 *Nature*, 273, 199–202, 1978.

567 Fabry, V., McClintock, J., Mathis, J. and Grebmeier, J.: Ocean acidification at high latitudes:
568 the bellwether, *Oceanography*, 22(4), 160–171, doi:10.5670/oceanog.2009.105, 2009.

569 Flynn, K. J., Blackford, J. C., Baird, M. E., Raven, J. A., Clark, D. R., Beardall, J., Brownlee,
570 C., Fabian, H. and Wheeler, G. L.: Changes in pH at the exterior surface of plankton with
571 ocean acidification, *Nat. Clim. Chang.*, 2(7), 510–513, 2012.

572 Furla, P., Galgani, I., Durand, I. and Allemand, D.: Sources and mechanisms of inorganic
573 carbon transport for coral calcification and photosynthesis., *J. Exp. Biol.*, 203 (22), 3445–57,
574 2000.

575 Gagnon, A. C., Adkins, J. F. and Erez, J.: Seawater transport during coral biomineralization,
576 *Earth Planet. Sci. Lett.*, 329-330, 150–161, doi:10.1016/j.epsl.2012.03.005, 2012.

577 Gazeau, F., Gattuso, J.-P., Greaves, M., Elderfield, H., Peene, J., Heip, C. H. R. and
578 Middelburg, J. J.: Effect of carbonate chemistry alteration on the early embryonic
579 development of the Pacific oyster (*Crassostrea gigas*), *PLoS One*, 6(8), e23010, 2011.

580 Glas, M. S., Fabricius, K. E., de Beer, D. and Uthicke, S.: The O_2 , pH and Ca^{2+}
581 microenvironment of benthic foraminifera in a high CO_2 world, *PLoS One*, 7(11), e50010,
582 2012a.

583 Glas, M. S., Langer, G. and Keul, N.: Calcification acidifies the microenvironment of a
584 benthic foraminifer (*Ammonia* sp.), *J. Exp. Mar. Bio. Ecol.*, 424-425, 53–58,
585 doi:10.1016/j.jembe.2012.05.006, 2012b.

586 Van Heuven, S., Pierrot, D., Rae, J. W. B., Lewis, E. and Wallace, D. W. R.: MATLAB
587 Program Developed for CO₂ System Calculations, , ORNL/CDIAC-105b, 2011.

588 Hofmann, G. E., Barry, J. P., Edmunds, P. J., Gates, R. D., Hutchins, D. A., Klinger, T. and
589 Sewell, M. A.: The effect of ocean acidification on calcifying organisms in marine
590 ecosystems: an organism-to-ecosystem perspective, *Annu. Rev. Ecol. Evol. Syst.*, 41, 127–
591 147, 2010.

592 Hönisch, B., Ridgwell, A., Schmidt, D. N., Thomas, E., Gibbs, S. J., Sluijs, A., Zeebe, R.,
593 Kump, L., Martindale, R. C., Greene, S. E., Kiessling, W., Ries, J., Zachos, J. C., Royer, D.
594 L., Barker, S., Marchitto, T. M., Moyer, R., Pelejero, C., Ziveri, P., Foster, G. L. and
595 Williams, B.: The geological record of ocean acidification., *Science*, 335(6072), 1058–1063,
596 doi:10.1126/science.1208277, 2012.

597 Jokiel, P. L.: Ocean acidification and control of reef coral calcification by boundary layer
598 limitation of proton flux, *Bull. Mar. Sci.*, 87(3), 639–657, doi:10.5343/bms.2010.1107, 2011a.

599 Jokiel, P. L.: The reef coral two compartment proton flux model: A new approach relating
600 tissue-level physiological processes to gross corallum morphology, *J. Exp. Mar. Bio. Ecol.*,
601 409(1-2), 1–12, doi:10.1016/j.jembe.2011.10.008, 2011b.

602 Jokiel, P. L.: Coral reef calcification: carbonate, bicarbonate and proton flux under conditions
603 of increasing ocean acidification, *Proc. R. Soc. B Biol. Sci.*, 280, 20130031, 2013.

604 Jokiel, P. L., Jury, C. P. and Rodgers, K. S.: Coral-algae metabolism and diurnal changes in
605 the CO₂-carbonate system of bulk sea water., *PeerJ*, 2, e378, doi:10.7717/peerj.378, 2014.

606 Jury, C. P., Whitehead, R. F. and Szmant, A. M.: Effects of variations in carbonate chemistry
607 on the calcification rates of *Madracis auretenra* (= *Madracis mirabilis* sensu Wells, 1973):
608 bicarbonate concentrations best predict calcification rates, *Glob. Chang. Biol.*, 16(5), 1632–
609 1644, 2010.

610 Keul, N., Langer, G., de Nooijer, L. J. and Bijma, J.: Effect of ocean acidification on the
611 benthic foraminifera *Ammonia* sp. is caused by a decrease in carbonate ion concentration,
612 *Biogeosciences*, 10(10), 6185–6198, doi:10.5194/bg-10-6185-2013, 2013.

613 Kleypas, J. A., Buddemeier, R. W., Archer, D., Gattuso, J.-P., Langdon, C. and Opdyke, B.
614 N.: Geochemical consequences of increased atmospheric carbon dioxide on coral reefs,
615 *Science*, 284(5411), 118–120, 1999.

616 Langer, G., Geisen, M., Baumann, K.-H., Kläs, J., Riebesell, U., Thoms, S. and Young, J. R.:
617 Species-specific responses of calcifying algae to changing seawater carbonate chemistry,
618 *Geochemistry, Geophys. Geosystems*, 7(9), doi:10.1029/2005GC001227, 2006.

619 Lee, S.-K., Boron, W. F. and Parker, M. D.: Substrate specificity of the electrogenic
620 sodium/bicarbonate cotransporter NBCe1-A (SLC4A4, variant A) from humans and rabbits.,
621 Am. J. Physiol. Renal Physiol., 304(7), F883–99, doi:10.1152/ajprenal.00612.2012, 2013.

622 Mackinder, L. C. M., Wheeler, G., Schroeder, D. C., Riebesell, U. and Brownlee, C.:
623 Molecular mechanisms underlying calcification in coccolithophores, Geomicrobiol. J., 27(6-
624 7), 585–595, 2010.

625 Mackinder, L., Wheeler, G., Schroeder, D., von Dassow, P., Riebesell, U. and Brownlee, C.:
626 Expression of biomineralization-related ion transport genes in *Emiliania huxleyi*., Environ.
627 Microbiol., 13(12), 3250–65, doi:10.1111/j.1462-2920.2011.02561.x, 2011.

628 Madshus, I. H.: Regulation of intracellular pH in eukaryotic cells, Biochem. J., 250, 1–8,
629 1988.

630 Mann, S.: Biomineralization: principles and concepts in bioinorganic materials chemistry,
631 Oxford University Press., New York, 2001.

632 Marubini, F., Ferrier-Pages, C., Furla, P. and Allemand, D.: Coral calcification responds to
633 seawater acidification: a working hypothesis towards a physiological mechanism, Coral
634 Reefs, 27(3), 491–499, 2008.

635 Melzner, F., Gutowska, M. A., Langenbuch, M., Dupont, S., Lucassen, M., Thorndyke, M. C.,
636 Bleich, M. and Pörtner, H.-O.: Physiological basis for high CO₂ tolerance in marine
637 ectothermic animals: pre-adaptation through lifestyle and ontogeny?, Biogeosciences, 6(10),
638 2313–2331, doi:10.5194/bg-6-2313-2009, 2009.

639 Millero, F. J.: Carbonate constants for estuarine waters, Mar. Freshw. Res., 61(2), 139–142,
640 2010.

641 Mucci, A.: The solubility of calcite and aragonite in seawater at various salinities,
642 temperatures, and one atmosphere total pressure, Am. J. Sci., 283(7), 780–799, 1983.

643 de Nooijer, L. J., Langer, G., Nehrke, G. and Bijma, J.: Physiological controls on seawater
644 uptake and calcification in the benthic foraminifer *Ammonia tepida*, Biogeosciences, 6(11),
645 2669–2675, doi:10.5194/bg-6-2669-2009, 2009.

646 de Nooijer, L. J., Spero, H. J., Erez, J., Bijma, J. and Reichart, G. J.: Biomineralization in
647 perforate Foraminifera, Earth-Science Rev., 135, 48–58, doi:10.1016/j.earscirev.2014.03.013,
648 2014.

649 Orr, J. C., Fabry, V. J., Aumont, O., Bopp, L., Doney, S. C., Feely, R. A., Gnanadesikan, A.,
650 Gruber, N., Ishida, A., Joos, F., Key, R. M., Keith, L., Maier-Reimer, E., Matear, R.,
651 Monfray, P., Mouchet, A., Najjar, R. G., Plattner, G.-K., Rodgers, K. B., Sabine, C. L.,
652 Sarmiento, J. L., Schlitzer, R., Slater, R. D., Totterdell, I. J., Weirig, M.-F., Yamanaka, Y. and
653 Yool, A.: Anthropogenic ocean acidification over the twenty-first century and its impact on
654 calcifying organisms, Nature, 437(7059), 681–686, 2005.

655 Paasche, E.: A review of the coccolithophorid *Emiliania huxleyi* with particular reference to
656 growth coccolith formation and calcification-photosynthesis interactions, *Phycologia*, 40(6),
657 503–529, 2002.

658 Pearse, V. B.: Incorporation of metabolic CO₂ into coral skeleton, *Nature*, 228, 383, 1970.

659 Peltola, E., Wanninkhof, R., Feely, R. A., D., H., Castle, R., Greeley, D., Zhang, J.-Z.,
660 Millero, J., Gruber, N., Bullister, J. L. and Graham, T.: Inorganic and organic carbon,
661 nutrient, and oxygen data from the R/V Ronald H. Brown repeat hydrography cruise in the
662 Atlantic ocean: CLIVAR CO₂ section A16N_2003a (4 June - 11 August, 2003)., 2003.

663 Pushkin, A. and Kurtz, I.: SLC4 base (HCO₃⁻, CO₃²⁻) transporters: classification, function,
664 structure, genetic diseases, and knockout models, *Am. J. Physiol. Physiol.*, 290(3), 580–599,
665 2006.

666 de Putron, S. J., McCorkle, D. C., Cohen, A. L. and Dillon, A. B.: The impact of seawater
667 saturation state and bicarbonate ion concentration on calcification by new recruits of two
668 Atlantic corals, *Coral Reefs*, 30(2), 321–328, 2011.

669 Ridgwell, A.: A Mid Mesozoic Revolution in the regulation of ocean chemistry, *Mar. Geol.*,
670 217(3-4), 339–357, doi:10.1016/j.margeo.2004.10.036, 2005.

671 Romero, M. F., Chen, A.-P., Parker, M. D. and Boron, W. F.: The SLC4 family of
672 bicarbonate transporters, *Mol. Aspects Med.*, 34(2), 159–182, 2013.

673 Rost, B., Riebesell, U., Burkhardt, S. and Sültemeyer, D.: Carbon acquisition of bloom-
674 forming marine phytoplankton, *Limnol. Oceanogr.*, 48(1), 55–67, 2003.

675 Schmittner, A., Oschlies, A., Matthews, H. D. and Galbraith, E. D.: Future changes in
676 climate, ocean circulation, ecosystems, and biogeochemical cycling simulated for a business-
677 as-usual CO₂ emission scenario until year 4000 AD, *Global Biogeochem. Cycles*, 22(1),
678 doi:10.1029/2007GB002953, 2008.

679 Schneider, K. and Erez, J.: The effect of carbonate chemistry on calcification and
680 photosynthesis in the hermatypic coral *Acropora eurystoma*, *Limnol. Oceanogr.*, 51(3),
681 1284–1293, 2006.

682 Schulz, K. G., Ramos, J. B., Zeebe, R. E. and Riebesell, U.: CO₂ perturbation experiments:
683 similarities and differences between dissolved inorganic carbon and total alkalinity
684 manipulations, *Biogeosciences*, 6, 2145–2153, 2009.

685 Schulz, K. G. and Riebesell, U.: Diurnal changes in seawater carbonate chemistry speciation
686 at increasing atmospheric carbon dioxide., *Mar. Biol.*, 160, 1889–1899, doi:10.1007/s00227-
687 012-1965-y, 2013.

688 Schulz, K. G., Riebesell, U., Rost, B., Thoms, S. and Zeebe, R. E.: Determination of the rate
689 constants for the carbon dioxide to bicarbonate inter-conversion in pH-buffered seawater
690 systems, *Mar. Chem.*, 100(1-2), 53–65, doi:10.1016/j.marchem.2005.11.001, 2006.

691 Sett, S., Bach, L. T., Schulz, K. G., Koch-Klavsen, S., Lebrato, M. and Riebesell, U.:
692 Temperature modulates coccolithophorid sensitivity of growth, photosynthesis and
693 calcification to increasing seawater pCO_2 ., *PLoS One*, 9(2), e88308,
694 doi:10.1371/journal.pone.0088308, 2014.

695 Shaw, E. C., Munday, P. L. and McNeil, B. I.: The role of CO_2 variability and exposure time
696 for biological impacts of ocean acidification, *Geophys. Res. Lett.*, 40(17), 4685–4688, 2013.

697 Sikes, C. S., Okazaki, K. and Fink, R. D.: Respiratory CO_2 and the supply of inorganic carbon
698 for calcification of sea urchin embryos, *Comp. Biochem. Physiol. Part A Physiol.*, 70(3), 285–
699 291, 1981.

700 Stumpp, M., Hu, M. Y., Melzner, F., Gutowska, M. A., Dorey, N., Himmerkus, N.,
701 Holtmann, W. C., Dupont, S. T., Thorndyke, M. C. and Bleich, M.: Acidified seawater
702 impacts sea urchin larvae pH regulatory systems relevant for calcification, *Proc. Natl. Acad.
703 Sci.*, 109, 18192–19197, 2012.

704 Takahashi, T., Olafsson, J., Goddard, J. G., Chipman, D. W. and Sutherland, S. C.: Seasonal
705 variation of CO_2 and nutrients in the high-latitude surface oceans: A comparative study,
706 *Global Biogeochem. Cycles*, 7(4), 843–878, 1993.

707 Tambutté, E., Tambutté, S., Segonds, N., Zoccola, D., Venn, A., Erez, J. and Allemand, D.:
708 Calcein labelling and electrophysiology: insights on coral tissue permeability and
709 calcification., *Proc. Biol. Sci.*, 279(1726), 19–27, doi:10.1098/rspb.2011.0733, 2012.

710 Tanaka, N., Monaghan, M. C. and Rye, D. M.: Contribution of metabolic carbon to mollusc
711 and barnacle shell carbonate, *Nature*, 320, 520–523, 1986.

712 Taucher, J. and Oschlies, A.: Can we predict the direction of marine primary production
713 change under global warming ?, *Geophys. Res. Lett.*, 38(January), 1–6,
714 doi:10.1029/2010GL045934, 2011.

715 Taylor, A. R., Brownlee, C. and Wheeler, G. L.: Proton channels in algae: reasons to be
716 excited., *Trends Plant Sci.*, 17(11), 675–84, doi:10.1016/j.tplants.2012.06.009, 2012.

717 Taylor, A. R., Chrachri, A., Wheeler, G., Goddard, H. and Brownlee, C.: A voltage-gated H^+
718 channel underlying pH homeostasis in calcifying coccolithophores., *PLoS Biol.*, 9(6),
719 e1001085, doi:10.1371/journal.pbio.1001085, 2011.

720 Thomsen, J., Gutowska, M. A., Saphörster, J., Heinemann, A., Trübenbach, K., Fietzke, J.,
721 Hiebenthal, C., Eisenhauer, A., Körtzinger, A., Wahl, M. and Melzner, F.: Calcifying
722 invertebrates succeed in a naturally CO_2 -rich coastal habitat but are threatened by high levels
723 of future acidification, *Biogeosciences*, 7(11), 3879–3891, 2010.

724 Thomsen, J., Haynert, K., Wegner, K. M. and Melzner, F.: Impact of seawater carbonate
725 chemistry on the calcification of marine bivalves, *Biogeosciences*, 12, 4209–4220,
726 doi:10.5194/bg-12-4209-2015, 2015.

727 Venn, A. A., Tambutté, E., Holcomb, M., Laurent, J., Allemand, D. and Tambutté, S.: Impact
728 of seawater acidification on pH at the tissue-skeleton interface and calcification in reef corals.,
729 Proc. Natl. Acad. Sci. U. S. A., 110(5), 1634–1639, doi:10.1073/pnas.1216153110, 2013.

730 Waldbusser, G. G., Hales, B., Langdon, C. J., Haley, B. A., Schrader, P., Brunner, E. L.,
731 Gray, M. W., Miller, C. a. and Gimenez, I.: Saturation-state sensitivity of marine bivalve
732 larvae to ocean acidification, Nat. Clim. Chang., 5, 273-280, doi:10.1038/nclimate2479, 2014.

733 Wanninkhof, R., Doney, S. C., Peltola, E., Castle, R., Millero, J., Bullister, J. L., D., H.,
734 Warner, M. J., Langdon, C., Johnson, G. C. and Mordy, C. W.: Carbon dioxide, hydrographic,
735 and chemical data obtained during the R/V Ronald H. Brown repeat hydrography cruise in the
736 Atlantic Ocean: CLIVAR CO₂ Section A16S_2005 (11 January - 24 February, 2005)., 2006.

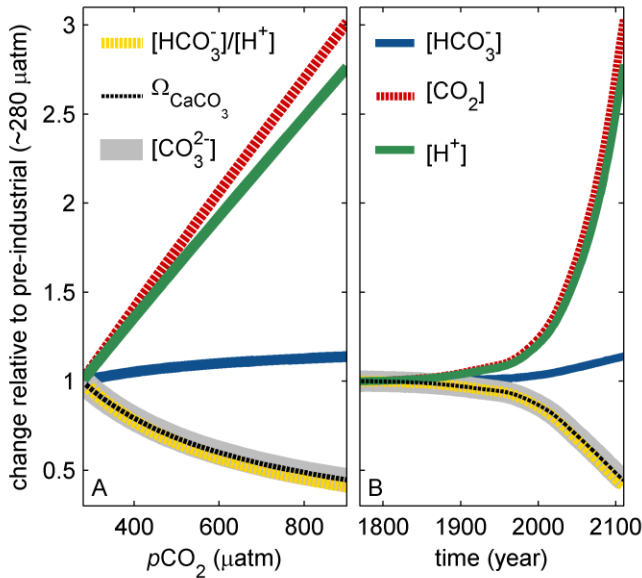
737 Weiner, S. and Addadi, L.: Crystallization pathways in biomineralization, Annu. Rev. Mater.
738 Res., 41, 21–40, 2011.

739 Wolf-Gladrow, D. and Riebesell, U.: Diffusion and reactions in the vicinity of plankton: a
740 refined model for inorganic carbon transport, Mar. Chem., 59(1), 17–34, 1997.

741 Zeebe, R. E. and Wolf-Gladrow, D. A.: CO₂ in seawater: Equilibrium, kinetics, isotopes,
742 Elsevier Oceanography Series, Amsterdam., 2001.

743

744

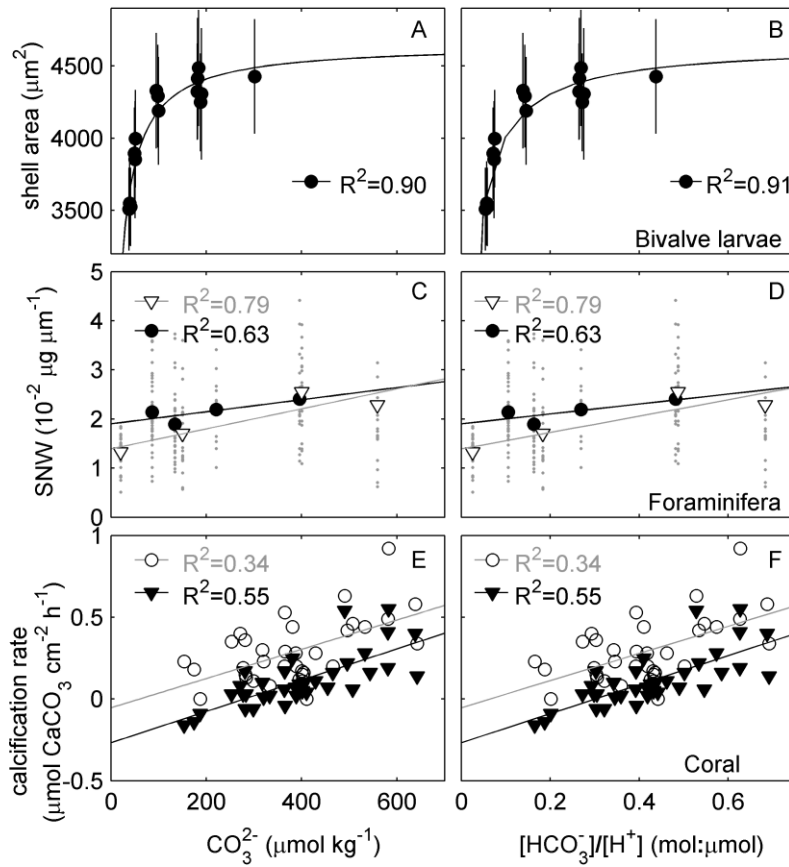


745

746

747 Figure 1. Change of different surface ocean carbonate chemistry parameters under “business-
 748 as-usual” climate change scenario SRES A2 with (A) increasing atmospheric pCO_2 and (B)
 749 over time. All changes are relative to the pre-industrial CO_2 partial pressure of ~ 280 μatm .
 750 Note that the slight deviations from proportionality between $[\text{CO}_3^{2-}]$, Ω_{CaCO_3} , and $[\text{HCO}_3^-]$
 751 $]/[\text{H}^+]$ are the result of changes in global average temperature and salinity in the course of
 752 climate change which affect K_2^* and K_{sp}^* (see section 3.5 for further details).

753

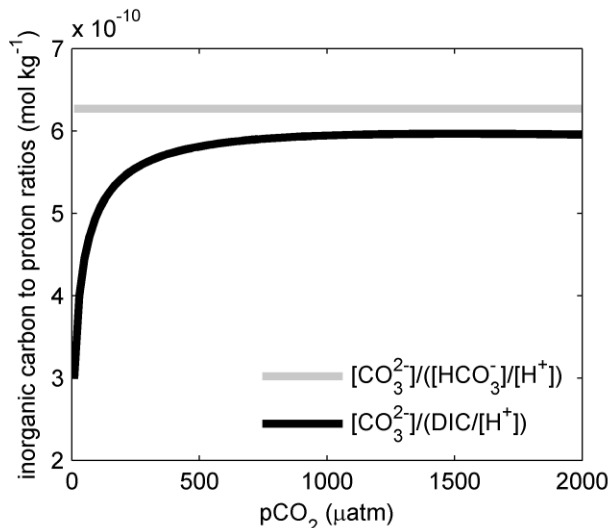


754

755

756 Figure 2. Correlations between calcification related measurements and $[CO_3^{2-}]$ (left panel) or
757 $[HCO_3^-]/[H^+]$ (right panel). (A, B) Shell areas of D-veliger larvae reached 3 days after
758 incubating embryos of the Pacific oyster *Crassostrea gigas* (Gazeau et al., 2011). (C, D) Size
759 normalized weight (SNW) of the foraminifer *Ammonia* spec. in its asexually reproducing life
760 cycle stage (Keul et al., 2013). Black dots: constant DIC, variable CO_2 . White triangles:
761 constant pH, variable CO_2 . (E, F) Calcification rates of the symbiont-bearing hermatypic coral
762 *Acropora eurystoma* (Schneider and Erez, 2006). White dots and black triangles refer to
763 incubations at light and dark, respectively.

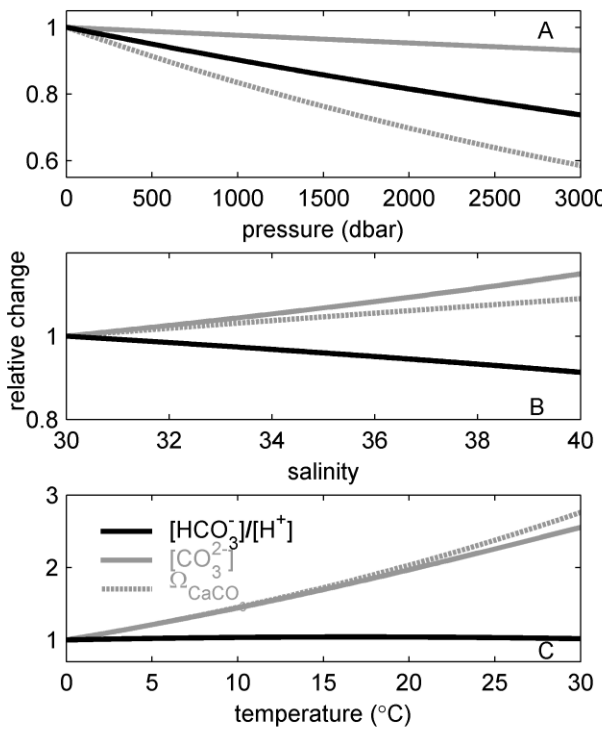
764



765

766

767 Figure 3. Ratio of $[\text{CO}_3^{2-}]$ and $[\text{HCO}_3^-]/[\text{H}^+]$ compared to the ratio of $[\text{CO}_3^{2-}]$ and $\text{DIC}/[\text{H}^+]$.
 768 $[\text{CO}_3^{2-}]/([\text{HCO}_3^-]/[\text{H}^+])$ is constant, since CO_3^{2-} and $[\text{HCO}_3^-]/[\text{H}^+]$ are proportional to each
 769 other under constant temperature, salinity and pressure (Eq. (9)). In contrast, the correlation
 770 between $[\text{CO}_3^{2-}]$ and $\text{DIC}/[\text{H}^+]$ only works well when the majority of DIC is found in the
 771 HCO_3^- pool. This is the case for pCO_2 values larger than ~ 250 - 500 μatm , where
 772 $[\text{CO}_3^{2-}]/(\text{DIC}/[\text{H}^+])$ shows very little change. Below this threshold, however, the correlation
 773 starts deviating from linearity since an exponentially increasing proportion of the DIC pool is
 774 present as CO_3^{2-} .
 775

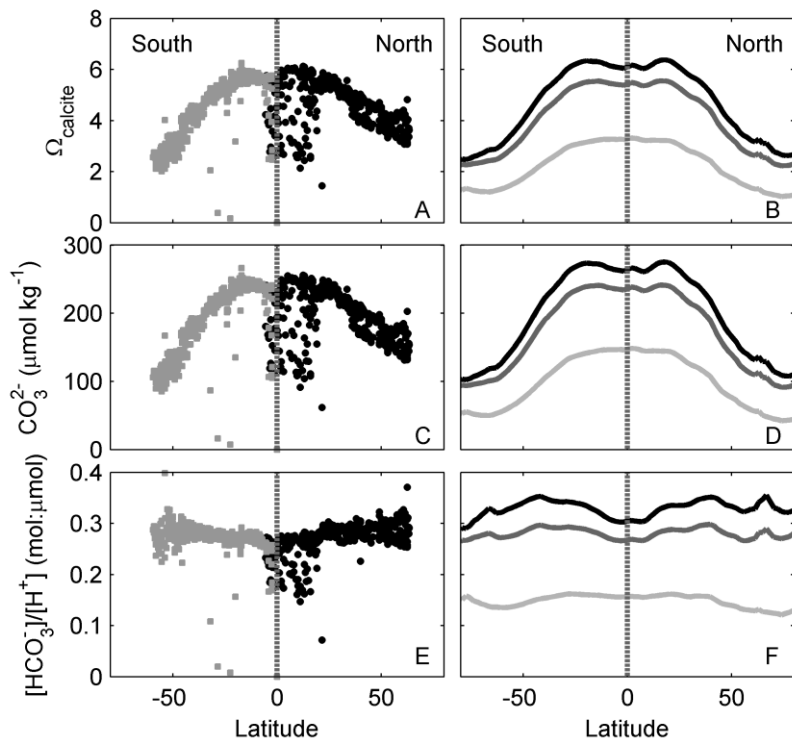


776

777

778 Figure 4. Relative change of $[\text{CO}_3^{2-}]$, Ω_{CaCO_3} , and $[\text{HCO}_3^-]/[\text{H}^+]$ on (A) a pressure gradient,
 779 (B) a temperature gradient, and (C) a salinity gradient.

780

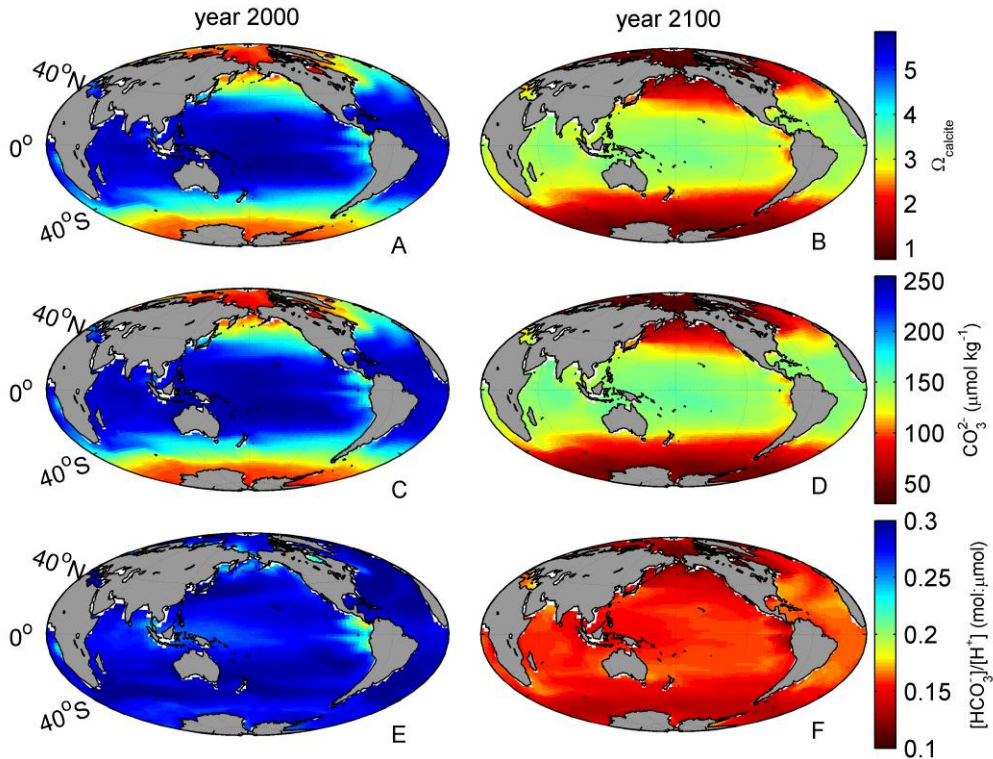


781

782

783 Figure 5. Change of Ω_{CaCO_3} , $[\text{CO}_3^{2-}]$, and $[\text{HCO}_3]/[\text{H}^+]$ in the surface ocean along a
 784 meridional gradient. The left panel (A, C, and E) shows compiled surface ocean (0 - 100 m)
 785 data from two north to south transects in the Atlantic, measured during CLIVAR CO₂ cruises
 786 in 2003 (black dots) and 2005 (grey squares), respectively. The right panel (B, D, and F)
 787 shows the latitudinal surface ocean (0 - 50 m) average calculated with the UVic model for the
 788 years 1770 (black line), 2000 (grey line), and 2100 (light grey line). The dotted vertical line
 789 illustrates the equator.

790

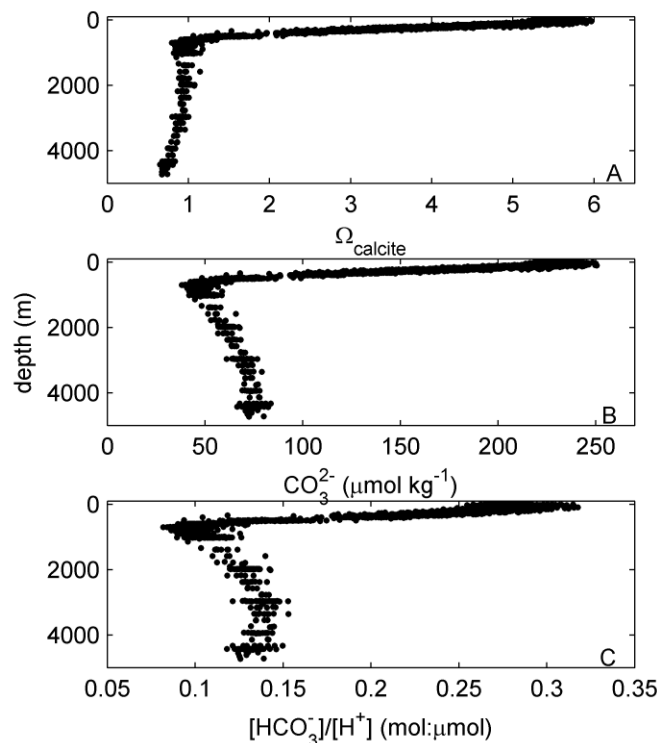


791

792

793 Figure 6. Surface ocean (0 – 50 m) Ω_{CaCO_3} (A, B), $[\text{CO}_3^{2-}]$ (C, D), and $[\text{HCO}_3^-]/[\text{H}^+]$ (E, F) in
 794 the year 2000 (left panel) compared to 2100 (right panel) calculated with the UVic model.
 795 The pronounced latitudinal gradient of Ω_{CaCO_3} and $[\text{CO}_3^{2-}]$ is absent in $[\text{HCO}_3^-]/[\text{H}^+]$ (see also
 796 Fig. 5). $[\text{HCO}_3^-]/[\text{H}^+]$ is quite homogeneous in 2000 and 2100 in all major ocean basins, with
 797 only some regional anomalies. These are found in some coastal areas (e.g. in the Bering Sea)
 798 and in eastern boundary upwelling systems, most noticeably off the west coast of South and
 799 Central America.

800



801

802

803 Figure 7. Change of (A) Ω_{CaCO_3} , (B) $[\text{CO}_3^{2-}]$, and (C) $[\text{HCO}_3^-]/[\text{H}^+]$ on a depth gradient at
 804 ALOHA time-series station near Hawaii ($22^\circ 45' \text{ N}$ $158^\circ 00' \text{ W}$). Compiled data from 1988 -
 805 2012 which was downloaded from the ALOHA website (<http://aco-ssds.soest.hawaii.edu/ALOHA/>).
 806

807

808